HHS Public Access

Author manuscript

Biol Psychiatry. Author manuscript; available in PMC 2016 July 15.

Published in final edited form as:

Biol Psychiatry. 2015 July 15; 78(2): 135–143. doi:10.1016/j.biopsych.2014.10.025.

Aberrant Cortical Morphometry in the 22q11.2 Deletion Syndrome

J. Eric Schmitt, MD PhD[1,2,°], **Simon Vandekar, BS**[1,°], **James Yi, MD PhD**[1,3], **Monica E. Calkins, PhD**[1], **Kosha Ruparel, MS**[1], **David R. Roalf, PhD**[1], **Daneen Whinna, BA**[1], **Margaret C. Souders, PhD CRNP**[4], **Theodore D. Satterwaite, MD**[1], **Karthik Prabhakaran, MS**[1], **Donna M. McDonald-McGinn, MS CGC**[4,5], **Elaine H. Zackai, MD**[4,5], **Ruben C. Gur, PhD**[1,2], **Beverly S. Emanuel, PhD**[4,5], and **Raquel E. Gur, MD PhD**[1,2,*]

[1]Brain Behavior Laboratory, Department of Psychiatry, Neuropsychiatry Section, University of Pennsylvania, Philadelphia, PA 19104, USA

[2]Department of Radiology, Hospital of the University of Pennsylvania, Philadelphia, PA 19104, USA

[3]Department of Child and Adolescent Psychiatry, Children's Hospital of Philadelphia, Philadelphia, PA 19104, USA

[4]Division of Human Genetics, Children's Hospital of Philadelphia, Philadelphia, PA 19104, USA

[5]Department of Pediatrics, Perelman School of Medicine, University of Pennsylvania, Philadelphia, PA 19104, USA

Abstract

Background—There is increased risk of developing psychosis in 22q11.2 deletion syndrome (22q11DS). Although this condition is associated with morphological brain abnormalities, simultaneous examination of multiple high-resolution measures of cortical structure has not been performed.

Methods—53 patients with 22q11DS, 30 with psychotic symptoms, were compared to demographically matched nondeleted youths: 53 typically developing and 53 with psychotic symptoms. High-resolution MRI measures of cerebral volume, cortical thickness, surface area, and an index of local gyrification (lGI) were obtained and compared between groups.

*Corresponding Author: Brain Behavior Laboratory, 10th Floor, Gates Building, Hospital of the University of Pennsylvania, Philadelphia, PA 19104, USA. raquel@mail.med.upenn.edu (R.E. Gur). Phone: (215) 662-2915, Fax: (215) 662-7903.

°Contributed equally to this manuscript

Financial Disclosure

Dr. RE Gur disclosed consulting to Otsuka America Pharmaceutical. Dr. RC Gur disclosed expert testimony. All other authors declare that they have no biomedical financial interest or potential conflict of interest.

Results—Patients with 22q11DS demonstrated global increases in cortical thickness associated with reductions in surface area, reduced lGI, and lower cerebral volumes relative to typically developing controls. Findings were principally in the frontal lobe, superior parietal lobes, and in the paramedian cerebral cortex. Focally decreased thickness was seen in the superior temporal gyrus and posterior cingulate cortex in 22q11DS relative to nondeleted groups. Patterns between nondeleted participants with psychotic symptoms and 22q11DS were similar, but with important differences in several regions implicated in schizophrenia. Post hoc analysis suggested that like the 22q11DS group, cortical thickness in nondeleted individuals with psychotic symptoms differed from typically developing controls in the superior frontal gyrus and superior temporal gyrus, two regions previously linked to schizophrenia.

Conclusions—Simultaneous examination of multiple measures of cerebral architecture demonstrates that differences in 22q11DS localize to regions of the frontal, superior parietal, superior temporal, and paramidline cerebral cortex. The overlapping patterns between nondeleted participants with psychotic symptoms and 22q11DS suggest partially shared neuroanatomic substrates.

Keywords

22q11 deletion syndrome; psychosis; cortical thickness; gyrification index; MRI; genetics

Introduction

The 22q11 deletion syndrome (22q11DS) is the most common known human genetic microdeletion, occurring in approximately 1:2000 live births (1). This hemizygous deletion at 22q11.2 spans ~3 Mb, although other deletions sizes are observed (2). The deletion results in a variable combination of craniofacial, cardiovascular, endocrine, and psychiatric abnormalities (1). Congenital heart disease has been reported in up to 70% of individuals including Tetralogy of Fallot, ventricular septal defects, and truncus arteriosus (1, 3). Cleft palate and other oropharyngeal abnormalities are common (4), as are pharyngeal and intracranial vascular abnormalities (1, 5, 6). Likewise more prevalent are thymic aplasia and diminished peripheral T-cells (7), hypothyroidism, hypoparathyroidism, and hypocalcemia (4).

The 22q11DS also imparts a significantly increased risk of intellectual disability and liability for several psychiatric disorders, most notably schizophrenia (8, 9); the presence of the 22q11DS is among the greatest known risk factors for psychosis (10, 11). Neuroimaging studies have sought to characterize functional neuroanatomy of 22q11DS as a genetically determined subtype of schizophrenia. Volumetric MRI studies have demonstrated global reductions in cerebral volumes compared to typically developing (TD) controls, with some studies suggesting relative sparing of the frontal lobes (12, 13). More recent studies have explored newer measures of cerebral morphometry such as cortical thickness (14–17), cerebral surface area (16), and measures of gyral complexity (18, 19). These reports have suggested increased frontal and inferior parietal cortical thickness and decreased thickness in the parieto-occipital region, decreased surface area in frontal and occipital lobes, and decreased gyral complexity in 22q11DS.

The current study represents a comprehensive high-resolution examination of the cerebral architecture of 22q11DS and nondeleted patients with psychotic symptoms using anatomic MRI. It also represents one of the largest studies of brain morphometry to date.

Methods and Materials

Sample

The 22q11DS sample was drawn from a prospective study, *Brain-Behavior and Genetic Studies of the 22q11DS* at University of Pennsylvania and Children's Hospital of Philadelphia (CHOP). Subjects were recruited from the "22q and You Center" at CHOP and through social media. Inclusion criteria were: age ≥ 8, English proficiency, estimated IQ>70 by clinical testing and the Wide Range Achievement Test IV (20), and stable medical status. Exclusion criteria were: pervasive developmental disorder or IQ<70, medical disorders that may affect brain function (e.g., uncontrolled seizures, head trauma, CNS tumor and infection) or visual performance (e.g., blindness). Subjects 12 years or older were eligible for MRI scanning.

Psychopathology was assessed with the Kiddie-Schedule for Affective Disorders and Schizophrenia (K-SADS)(21), Structured Interview for Prodromal Syndromes (SIPS)(22), and the psychotic and mood differential diagnoses modules of the Structured Clinical Interview for DSM-IV (Modules C and D)(23). As detailed previously (20), positive, negative and disorganized symptoms were rated on the 7-point Scale of Prodromal Symptoms (SOPS) from the SIPS (22) (0 - "absent," 1 -"questionably present," 2 - "mild," 3 - " moderate," 4 - "moderately severe," 5 -"severe but not psychotic," and 6 - "severe and psychotic"). A prodrome diagnosis was given if a patient had one positive symptom rated ≥ 3 or at least two negative and/or disorganized symptoms rated ≥ 3 within the past 6 months. The 22q11DS psychosis spectrum group included those with the prodrome diagnoses and psychiatric disorders with psychotic symptoms (schizophrenia, psychosis not otherwise specified, major depression with psychotic features, schizoaffective disorder, and delusional disorder).

Deletion status was confirmed using multiplex ligation dependent probe amplification (24). Penn and CHOP IRBs approved all procedures. Informed consent/assent was obtained from each participant and accompanying parent, for those younger than 18 at the time of initial evaluation.

Control groups were obtained from the Philadelphia Neurodevelopmental Cohort (PNC), a prospective neuroimaging sample of 1400 youths aged 8–21 years (25–27). An automated optimal matching algorithm developed by Kosanke and Bergsralh (GREEDY) written in SAS (SAS Institute, Cary NC) generated a 1:1 typically developing (ND-TD) subsample from this population matched to the 22q11DS sample based on age, race, and gender (28). A second subsample of subjects from the PNC with psychosis spectrum symptoms (ND-PS) was obtained and similarly matched using an automated algorithm. Psychosis spectrum symptoms were assessed using an abbreviated K-SADS and scales for measuring subthreshold psychotic symptoms including the PRIME Screen-Revised and selected SOPS scales (21, 26, 27). Summary group statistics are provided in Table 1.

Image Acquisition

High-resolution axial T1 weighted magnetization prepared rapid acquisition gradient echo was acquired, with the following parameters; TR/TE 1810/3.51 ms; TI 1100 ms; FOV 180 × 240 mm; effective resolution 1 mm3. Subjects were scanned on the same 3T MRI scanner (TIM Trio; Siemens, Erlangen, Germany) using a 32-channel head coil by a board certified technologist.

Image processing

DICOM Images were imported into FreeSurfer version 5.0, a freeware image-processing program (http://surfer.mgh.harvard.edu). FreeSurfer's surface-based image processing pipeline has been described (29–32). Briefly, for each subject, image intensity was normalized to account for magnetic field inhomogeneity. The skull and other non-brain tissues were removed (33). Preliminary segmentation was then performed using a connected components algorithm. The surface boundary was then covered with a polygonal tessellation and smoothed, resulting in high-resolution vertices over both cerebral hemispheres. A deformable surface algorithm was then employed to identify the pial surface. For all subjects, the cortical surface model was manually reviewed and edited if necessary.

Cerebral volume (CV), cortical thickness (CT), surface area (SA), and local gyrification index (lGI) were subsequently calculated at high-resolution. Cortical thickness is estimated as the distance between the pial surface and the gray-white matter junction (31). Surface area was calculated by measuring the average triangular size surrounding the tesselatted cortical vertices, following deformation of individual subject vertices (32, 34). Maps of cerebral volume could then be generated by calculating the product of SA and CT at each vertex.

Gyrification index was determined using a method originally described by Schaer et al. (19) for evaluating gyral complexity in 22q11DS and subsequently integrated into FreeSurfer. Briefly, this method creates a smoothed outer surface surrounding the more convoluted pial surface at every vertex. The algorithm then calculates the ratio of the inner and outer surfaces for *j* faces in the 3D mesh:

$$GI|_{3D} = \frac{\sum_{j=1}^{M_P} A_P^j}{\sum_{j=1}^{M_O} A_O^j}$$

where A_P^j and A_O^j represent the pial and outer (smoothed) surfaces, respectively, and M_P and M_0 represent the total number of faces in the pial and outer mesh.

Statistical Analyses

Measures of total cortical volume, total surface area, mean cortical thickness, and mean lGI were calculated to identify global group differences in cerebral morphology. ANOVA was performed with diagnostic group as an independent factor controlling for linear and nonlinear effects of age, sex, and race. Post-hoc Tukey-Kramer tests were employed to identify which groups drove global differences.

Three group ANOVAs were then performed at each vertex for CT in order to identify significant group differences, controlling for linear and nonlinear effects of age, sex, and race. Control for multiple testing was performed using false discovery rate (FDR), with a threshold of q=0.05 (35). Univariate ANOVA probability maps were similarly constructed for measures of SA, CB, and lGI. Post-hoc pairwise t-tests were performed to identify which group contrasts were driving the observed differences in brain measures. Control of multiple testing was performed via FDR.

To explore the relationships between 22q11DS and psychosis, we performed subgroup analyses comparing the 30 22q11DS subjects with psychosis spectrum symptoms to their matches from the ND-TD and ND-PS groups (Table 1S). Post-hoc pairwise tests were similarly performed on the full group models. We similarly contrasted cerebral measures between the 22q11DS subjects with and without psychosis spectrum symptoms (Table 2S).

To increase sensitivity for subtle group differences (particularly between the two nondeleted groups), we reanalyzed the data using cluster threshold permutation methods rather than FDR to control for multiple testing (33–35). These methods, adapted for surface based anatomical analysis from methods originally designed for fMRI data, are built into the Freesurfer environment. They use permutation to estimate maximum cluster size assuming that false positive vertices are less likely to be near each other; thus unlike FDR, cluster thresholding takes advantage of spatial information inherent to imaging data. The cluster thresholding approach does sacrifice spatial specificity relative to FDR, in return for an increased sensitivity for small but more regional group differences. For these analyses, a full width half maximum (FWHM) of 20 with 5000 permutations and global p-value threshold of 0.05 was used to identify significant clusters. Post hoc statistical testing of pairwise group differences was then performed, with control of multiple testing via the Tukey-Kramer test.

Results

Global Measures

Patients with 22q11DS had significantly reduced total cortical volumes relative to nondeleted controls (Table 2). These reductions were driven by global reductions in total brain area rather than reductions in cortical thickness. Indeed, global measures of thickness were significantly *increased* in 22q11DS relative to controls. Mean lGI was decreased in the 22q11DS group. Statistically significant group differences were identified for all four global measures, with p-values <0.0009. Global differences were primarily driven by differences in deletion status; there were no significant differences between the TD and PS groups. Vertex level ANOVA demonstrated that significant differences in all measures were heterogeneous throughout the cerebrum (Figure 1), with the midline cortex and frontal and superior parietal lobes particularly affected.

Cerebral Volume

Subjects with 22q11DS had multiple foci of significantly lower cerebral volume relative to ND-TD (Figure 2); differences were centered on the rostral lateral frontal lobe, superior parietal lobe, medial occipital lobe, and temporal pole. Relative volumetric increases were

observed in the insular cortex bilaterally in 22q11DS relative to ND-TD. Similar but less extensive differences were seen when comparing 22q11DS and ND-PS groups. An exception was a focal region of bilaterally decreased volume in the caudal frontal lobe in ND-PS relative to 22q11DS. There were no significant differences between 22q11DS subjects with and without psychosis spectrum symptoms or between the ND-TD and ND-PS groups after adjusting for multiple testing.

Cortical Thickness

Thicker cortex was seen in 22q11DS relative to the ND-TD group in frontal lobes bilaterally, orbitofrontal cortex bilaterally extending into anterior insula and operculum, in inferior parietal lobe and paracentral lobule, fusiform gyrus, cuneus and paracalcarine cortex (Figure 2). In contrast, significantly lower cortical thickness in 22q11DS was observed in anterior and mid superior temporal gyrus and mid to posterior cingulate gyrus bilaterally. Similar patterns were seen for the 22q11DS compared to ND-PS. However, we observed additional foci of significantly greater thickness in 22q11DS in left dorsolateral prefrontal cortex and right insula, and less pronounced decreases in superior temporal cortex and medial frontal lobes. Direct comparison between ND-TD and ND-PS groups did not demonstrate significant findings at vertex level. Similarly, no significant differences in cortical thickness were seen between 22q11DS subjects with and without psychosis spectrum, after controlling for multiple testing with FDR.

Clusterwise correction identified 10 significant clusters (Figure 3). For clusters in the parietal and occipital lobe, group differences were driven by significantly thicker cortex in 22q11DS compared to the two control groups. In contrast, a cluster including portions of the left superior frontal gyrus (SFG), anterior cingulate, and medial orbitofrontal cortex was more complex, with significant differences between all groups and with the ND-PS intermediate in thickness between the other two groups. A similar pattern was seen in left superior temporal lobe (STG). In right STG, there were significant group decreases in the ND-PS group relative to ND-TD ($p=0.001$). The results from cluster analyses for cerebral volume, surface area, and local gyrification index are presented in Supplement (Figure 2S).

Surface Area

Analysis of cerebral surface area identified multiple areas that were significantly smaller in 22q11DS relative to TD (Figure 2). On the lateral surface, rostral frontal lobes, superior parietal lobe, and lingual gyrus were particularly affected bilaterally. Midline areal differences were more extensive than those of cortical thickness, with large portions of the medial superior frontal gyrus, anterior cingulate cortex, and midline occipital lobe affected bilaterally. Similar findings were seen comparing 22q11DS to the ND-PS group at the vertex level, with less extensive differences in the lateral temporal lobe relative to the 22q11DS compared to ND-TD contrast. There were no significant differences between ND-TD and ND-PS groups or between 22q11DS subjects with and without psychosis spectrum. Cluster models produced similar patterns; group differences were entirely driven by areal decreases in 22q11DS relative to ND-TD; there were no significant differences between ND-PS and 22q11DS.

Local Gyrification Index (lGI)

Analysis of lGI demonstrated group differences in gyral complexity (Figure 2). Smaller lGIs were noted in 22q11DS throughout anterior and posterior midline cerebral cortex, in orbitofrontal cortex and frontal pole, centered over angular gyrus and extending into the remainder of the inferior parietal lobe, and mid pre-and postcentral gyrus. Similar to surface area, group differences were principally explained by deletion status. Cluster threshold models produced similar findings, with significant decreases in mean lGI ($p < 0.0001$) between 22q11DS and other groups in all cases.

Discussion

Although schizophrenia is a devastating condition with significant morbidity and mortality, the underlying biological manifestations remain elusive. Twin and family studies have demonstrated a strong genetic influence on liability to develop schizophrenia (10) and large scale genetic studies have begun to identify putative genes, most with very small effect sizes (36). Understanding the neural substrates of this genetic variation remains an area of active research. 22q11DS represents the genetic variant of largest effect on liability to schizophrenia, and thus warrants investigation.

Our study provides a comprehensive examination of morphological characteristics of 22q11DS in a relatively large sample at high resolution and high field-strength. Our findings replicate observed patterns of volumetric reductions in parieto-occipital cortex, dorsolateral prefrontal cortex, and midline structures, with relative increases in insular volumes compared to the ND-TD (12, 15, 16, 37, 38). In 22q11DS, we additionally identified significantly thicker cortex in the frontal lobes, inferior parietal lobes, lingual gyrus, and medial occipital lobes. Higher cortical thickness in these regions was associated with corresponding smaller mean surface area. The observed patterns of areal reduction in 22q11DS were similar to, but more extensive than for the observed increases in cortical thickness. We also observed extensive midline, frontal, and parietal reductions in cortical gyral complexity relative to ND-TD controls.

A similar approach by Jalbrzikowski et al., simultaneously examined differences in cortical thickness, surface area, and volume in a sample of 31 individuals with 22q11DS (mean age 16.4) and 34 matched ND-TD controls (16), also at 3T. FreeSurfer analysis of 60 cortical regions of interest identified volumetric reductions in frontal lobes, anterior cingulate, cuneus, precuneus, superior parietal and temporal cortex. Like the current study, the volumetric differences were primarily driven by decreases in cortical surface area. Also similar to the current study, they observed relatively *thickened* cortex in 22q11DS, most pronounced in frontal lobes. Thus, higher cortical thickness may explain why early volumetric studies observed relative preservation of the frontal lobe (12) despite the observed large reductions in area. Schaer et al. similarly reported increased cortical thickness in frontal regions in a large sample of children and adolescence with 22q11DS (14). However, in this longitudinal study deviant trajectories of cortical thickness were observed in 22q11DS compared to ND-TD; while dorsal frontal regions were thicker in 22q11DS during late childhood and adolescence, by adulthood thickness in these regions were comparable to ND-TD (group by age interaction). Schaer et al. also observed this

interaction in left superior temporal gyrus; although there were no significant group differences in younger subjects, relative decreases in this region manifested by adulthood in 22q11DS (14).

Unlike elsewhere in the brain, we also observed significant *reductions* in cortical thickness within superior temporal lobes and in mid-cingulate gyrus bilaterally in 22q11DS. Several prior studies on 22q11DS suggested morphological deficits in superior temporal gyrus. Jalbrzikowski et al. observed reductions in superior temporal lobes in their ROI analysis, although the findings did not reach statistical significance (16). Eliez et al. identified significant reductions in hand-drawn superior temporal gyrus volumes in 23 children and adolescents with 22q11DS compared to matched ND-TD; these differences were not significant after adjusting for global brain volume (39). Aberrant morphology of STG has long been associated with schizophrenia (40), with recent studies showing reductions in both gray matter density and cortical thickness (41, 42). A large study by Chow et al. on subjects with 22q11DS demonstrated significant reductions in STG gray matter density in the group with schizophrenia (43), a finding particularly interesting given that STG morphological abnormalities have been associated with idiopathic schizophrenia.

To further characterize the neurodevelopmental patterns in 22q11DS, we examined differences in gyral complexity using the local gyrification index (lGI). We identified smaller lGI in 22q11DS, primarily in the paramidline cerebral cortex and extending to the superior and lateral parietal cortices. Decreases in gyrification in frontal and parietal lobes have been reported in several studies at lower levels of resolution (18, 44). Prior studies of gyral complexity at vertex level are limited. For example, Schaer et al. examined lGI in 44 young individuals with 22q11DS (mean age 9.1 years) and also identified significantly smaller lGIs in orbitofrontal cortex, superior parietal lobes extending into the angular gyri, and midline structure including the cingulate cortex and midline parietal and occipital lobes (45). Likewise, Srivastra et al. examined lGI in 49 children with 22qDS (mean age 10.74 years) and found lower measures of gyral complexity in midline structures and within the parietal lobes and orbito frontal cortices (46). Although our findings suggest more extensive changes in the midline frontal lobes, the overall pattern of findings is strikingly similar to these prior reports.

Considered together, the overlapping patterns of generally thicker cortex, smaller surface area, and reduced gyral complexity are suggestive of aberrant neural organization and migration in 22q11DS, most pronounced in the frontal and parietal lobes and midline occipital lobe. Thickened cortex compared to ND-TD controls is an unusual finding in the literature, although it has been reported with other neurodevelopmental conditions including Williams syndrome (47), autism (48, 49), and both idiopathic polymicrogyria and lissencephaly (50, 51). Notably, neuropathologic correlation in 22q11DS is limited, with a single case series demonstrating extensive microscopic gray matter heterotopia in 1 of 3 specimens (52). Qualitative MRI studies have reported pachygyria and polymicrogyria (abnormalities of migrational and postmigrational neuronal development, respectively) in 22q11DS (53, 54), findings that may relate to the quantitative reductions in lGI found in the current study. Although qualitative reports of polymicrogyria have not noted as extensive or

consistent findings compared to newer quantitative measures, differences are likely due to increased sensitivity of these new measures to detect more subtle abnormalities.

The potential etiologies of polymicrogyria are myriad and include genetic, metabolic, infectious, and traumatic causes (55). However, it is hypothesized that most are ultimately caused by vascular injury resulting in disruption of cellular interactions at the glial-pial barrier (51). A putative vascular cause of neuromigrational abnormalities is a particularly intriguing hypothesis in 22q11DS, given the spectrum of cardiovascular features associated with the condition(1). Schaer et al. have described an association between congenital heart disease and gyrification at the parieto-temporal-occipital junction (56), although the reason for this association is incompletely understood. Ongoing genetically-mediated cerebrovascular insult could potentially explain both the observed congenital neuroanatomic abnormalities and the aberrant neurodevelopmental trajectories observed later in life (14, 16, 46). 22q11DS is associated with diffuse white matter abnormalities reminiscent of small vessel ischemic changes, findings often seen in healthy people following middle age (57–59). Limited pathological examination of individuals with 22q11DS has demonstrated astrocytic gliosis and hemosiderin-laden macrophages in cerebral white matter, suggestive of diffuse cerebrovascular injury consistent with small vessel ischemia (52) in 2 out of 3 specimens examined.

Morphometric Relationships to Psychosis Spectrum Symptoms

Our purely vertex-level analysis did not identify any direct differences between subgroups with and without psychosis spectrum symptoms after controlling for multiple testing. This may be due to our relatively small sample, and possibly the relatively broad definition of the psychosis spectrum in our ND-PS group. The broad definition permitted power to establish differences between individuals with psychotic symptoms and those without across deletion groups. As our 22q11DS sample grows, we will be able to examine whether individuals with more severe psychotic symptoms have more specific patterns of abnormalities. It is important to note that in our efforts to control for type I error we are at risk for committing a type II error and therefore should await the availability of larger samples before concluding that such differences do not exist.

We did observe indirect vertex level differences between our ND-TD and ND-PS groups, as there were significant differences in their probability maps when each was compared to the 22q11DS group. In particular, the ND-PS group had more extensive cortical thickness reductions in the dorsolateral prefrontal cortex relative to 22q11DS, but less extensive thickness differences elsewhere in the brain including the superior temporal gyrus and superior frontal lobe. Post hoc cluster threshold models did identify significant reductions in right STG in ND-TD relative to ND-PS and SFG thickness intermediate between 22q11DS and ND-TD groups, suggesting a partially shared neural etiology for psychosis. The ND-PS group also tended towards less extensive differences in area compared to 22q11DS, particularly in the temporal lobes.

The literature on anatomic differences in schizophrenia is variable, but volume and cortical thickness reductions in dorsolateral prefrontal cortex, limbic and midline structures, and mesial temporal structures are most commonly reported (42, 60–65). Unlike the prior

literature on schizophrenia, the current study focuses on subthreshold psychotic symptoms, which may explain the more subtle findings we observed relative to the schizophrenia literature. There is mounting evidence that neurodegeneration during late childhood and adolescence is evident at the onset of schizophrenia in susceptible individuals; patients with schizophrenia experience loss of cortical thickness and volume over time when examined longitudinally (66). It is possible that our ND-PS subjects represent individuals experiencing early neurodegenerative changes that are difficult to detect when compared to typically developing controls directly. Subtle differences in ND-PS groups (for example in dorsolateral prefrontal cortex and superior temporal gyrus) may become more apparent when the 22q11DS contrast is added. Although our findings are preliminary, the approach of group triangulation may ultimately help to disentangle what portions of the 22q11DS endophenotype are shared with idiopathic schizophrenia. Longitudinal studies using this multiple group approach may prove particularly fruitful for identifying putative biomarkers present prior to the manifestation of florid psychosis.

Although the current study supports several prior findings on 22q11DS in a relatively large sample, there are several limitations of the study that must be noted. First, our subject ascertainment procedures selected for higher functioning patients. Thus, the study may underestimate morphological differences between the 22q11DS and the nondeleted groups. Similarly, our study excluded patients with neurological diagnoses, including seizure disorders. Considering that seizures are associated with neurodevelopmental abnormalities, this selection criteria again may underestimate true group differences as compared to an unselected sample (55). Secondly, although ND-TD and 22q11DS were matched for age, gender, and race, the 22q11DS groups were still significantly older. Age, along with race and gender, was partially controlled statistically in our analyses. Thirdly, our PNC screening procedure for psychotic symptomology is less comprehensive as compared to the 22q11DS group. Finally, there were differences in the prevalence of mood disorders between 22q11DS subjects with and without psychosis spectrum symptoms, which could potentially affect the contrast between these subgroups.

Conclusions

Comprehensive analysis of multiple complementary measures of cerebral architecture in 22q11DS demonstrate overlapping abnormalities in cortical thickness, surface area, and local gyrification, most notably in the frontal, superior parietal, and paramidline cerebral cortex. Findings suggest a neurodevelopmental origin of many of the neuroanatomic manifestations of 22q11DS. Several affected regions are associated with idiopathic schizophrenia in the literature, most strikingly in the superior temporal gyrus, and prefrontal cortex, with our study providing preliminary evidence that subjects with idiopathic psychotic symptoms may have somewhat different morphological patterns than ND-TD controls when compared to 22q11DS. By identifying the neuroanatomic “fingerprint” of a deletion we can elucidate the contribution of specific genetic effects to the phenotypic manifestations of psychosis. This paradigm can extend to other populations with genetic alterations associated with increased risk for psychosis, thereby establishing both shared and unique biomarkers for at risk populations.

Supplementary Material

Refer to Web version on PubMed Central for supplementary material.

Acknowledgements

This study was supported by NIH grants MH087626, MH087636, and T32 grants MH019112 (JJY), EB004311 (JES), and an RSNA Fellow Grant (JES). The Philadelphia Neurodevelopmental Cohort is supported by NIH grants MH089983 and MH089924. Additional support was provided by K23MH098130 (TDS), K08MH079364 (MEC), and the Marc Rapport Family Investigator grant through the Brain and Behavior Foundation (TDS).

References

1. Shprintzen RJ. Velo-cardio-facial syndrome: 30 years of study. Develop Disabil Res Rev. 2008; 14:3–10.
2. Shaikh TH, Kurahashi H, Saitta SC, O'Hare AM, Hu P, Roe BA, et al. Chromosome 22-specific low copy repeats and the 22q11.2 deletion syndrome: genomic organization and deletion endpoint analysis. Hum Molec Genet. 2000; 9:489–501. [PubMed: 10699172]
3. Ryan AK, Goodship JA, Wilson DI, Philip N, Levy A, Seidel H, et al. Spectrum of clinical features associated with interstitial chromosome 22q11 deletions: a European collaborative study. J Med Genet. 1997; 34:798–804. [PubMed: 9350810]
4. Bassett AS, Chow EWC, Husted J, Weksberg R, Caluseriu O, Webb GD, Gatzoulis MA. Clinical features of 78 adults with 22q11 Deletion Syndrome. Am J Med Genet Part A. 2005; 138:307–313. [PubMed: 16208694]
5. MacKenzie-Stepner K, Witzel M, Stringer D, Lindsay W, Munro I, Hughes H. Abnormal carotid arteries in the velocardiofacial syndrome: A report of three cases. Plast Reconstruct Surgery. 1987; 80:347–351.
6. Mitnick R, Bello J, Golding-Kushner K, Argamaso R, Shprintzen R. The use of magnetic resonance angiography prior to pharyngeal flap surgery in patients with velocardiofacial syndrome. Plast Reconstruct Surgery. 1996; 97:908–919.
7. Jawad F, McDonald-Mcginn DM, Zackai E, Sullivan KE. Immunologic features of chromosome 22q11.2 deletion syndrome (DiGeorge syndrome/velocardiofacial syndrome). J Pediatrics. 2001; 139:715–723.
8. Murphy KC, Jones LA, Owen MJ. High rates of schizophrenia in adults with velo-cardio-facial syndrome. Arch Gen Psychiatry. 1999; 56:940–945. [PubMed: 10530637]
9. Bassett A, Chow E. 22Q11 deletion syndrome: A genetic subtype of schizophrenia. Biol Psychiatry. 1999; 46:882–891. [PubMed: 10509171]
10. Sullivan PF, Kendler KS, Neale MC. Schizophrenia as a complex trait. Arch Gen Psychiatry. 2014; 60:1187–1192. [PubMed: 14662550]
11. Giusti-rodríguez P, Sullivan PF. The genomics of schizophrenia?: update and implications. J Clin Investigation. 2013; 123:4557–4563.
12. Eliez S, Schmitt JE, White CD, Reiss AL. Children and adolescents with velocardiofacial syndrome: A volumetric MRI study. Am J Psychiatry. 2000; 157:409–415. [PubMed: 10698817]
13. Tan GM, Arnone D, McIntosh AM, Ebmeier KP. Meta-analysis of magnetic resonance imaging studies in chromosome 22q11.2 deletion syndrome (velocardiofacial syndrome). Schizoph Res. 2009; 115:173–181.
14. Schaer M, Debbané M, Bach Cuadra M, Ottet M-C, Glaser B, Thiran J-P, Eliez S. Deviant trajectories of cortical maturation in 22q11.2 deletion syndrome (22q11DS). a cross-sectional and longitudinal study. Schizoph Res. 2009; 115:182–190.
15. Bearden CE, van Erp TGM, Dutton RA, Tran H, Zimmermann L, Sun D, et al. Mapping cortical thickness in children with 22q11.2 deletions. Cereb Cortex. 2007; 17:1889–1898. [PubMed: 17056649]
16. Jalbrzikowski M, Jonas R, Senturk D, Patel A, Chow C, Green MF, Bearden CE. Structural abnormalities in cortical volume, thickness, and surface area in 22q11.2 microdeletion syndrome:

Relationship with psychotic symptoms. NeuroImage Clinical. 2013; 3:405–415. [PubMed: 24273724]

17. Bearden CE, van Erp TGM, Dutton RA, Lee AD, Simon TJ, Cannon TD, et al. Alterations in midline cortical thickness and gyrification patterns mapped in children with 22q11.2 deletions. Cereb Cortex. 2009; 19:115–126. [PubMed: 18483006]
18. Schaer M, Schmitt JE, Glaser B, Lazeyras F, Delavelle J, Eliez S. Abnormal patterns of cortical gyrification in velo-cardio-facial syndrome (deletion 22q11.2): an MRI study. Psychiatry Res. 2006; 146:1–11. [PubMed: 16388934]
19. Schaer M, Cuadra MB, Tamarit L, Lazeyras F, Eliez S, Thiran J, Member S. A surface-based approach to quantify local cortical gyrification. IEEE Transactions on Medical Imaging. 2008; 27:161–170. [PubMed: 18334438]
20. Wilkinson, G.; Robertson, G. Wide range achievement test: Fourth edition. Lutz, FL: Psychological Assessment Resources; 2006.
21. Kaufman J, Birmaher B, Brent D, Rao U, Flynn C, Moreci P, et al. Schedule for affective disorders and schizophrenia for school-age children-present and lifetime version (K-SADS-PL): Initial reliability and validity data. J Am Acad Child Adoles Psychiatry. 1997; 36:980–988.
22. Miller TJ, McGlashan TH, Rosen JL, Cadenhead K, Cannon T, Ventura J, et al. Prodromal assessment with the structured interview for prodromal syndromes and the scale of prodromal symptoms: predictive validity, interrater reliability, and training to reliability. Schizophr Bull. 2003; 29:703–715. [PubMed: 14989408]
23. First M, Gibbon M. Hilsenroth M, Segal D. The structured clinical interview for DSM-IV axis I disorders (SCID-I) and the structured clinical interview for DSM-IV axis II disorders (SCID-II). Comprehensive Handbook of Psychological Assessment, Volume 2: Personality Assessment. 2004:134–143.
24. Jalali GR, Vorstman JAS, Errami A, Vijzelaar R, Biegel J, Shaikh T, Emanuel BS. Detailed analysis of 22q11.2 with a high density MLPA probe set. Hum Mutation. 2008; 29:433–440.
25. Satterthwaite TD, Elliott MA, Ruparel K, Loughead J, Prabhakaran K, Calkins ME, et al. Neuroimaging of the Philadelphia neurodevelopmental cohort. NeuroImage. 2013; 86:544–553. [PubMed: 23921101]
26. Calkins M, Moore T, Merikangas K, Berstein M, Satterthwaite T, Bilker W, et al. The psychosis spectrum in a young U.S. community sample: Findings from the Philadelphia neurodevelopmental cohort. World Psychiatry. in press.
27. Gur RC, Calkins ME, Satterthwaite TD, Ruparel K, Bilker WB, Moore TM, et al. Neurocognitive growth charting in psychosis spectrum youths. JAMA Psychiatry. 2014; 71:366–374. [PubMed: 24499990]
28. Kosanke, J.; Bergstralh, E. Match one or more controls to cases using the GREEDY algorithm. Rochester, MN: Mayo Clinic College of Medicine; 2004.
29. Dale AM, Fischl B, Sereno MI. Cortical surface-based analysis. NeuroImage. 1999; 194:179–194. [PubMed: 9931268]
30. Fischl B. FreeSurfer. NeuroImage. 2012; 62:774–781. [PubMed: 22248573]
31. Fischl B, Dale A. Measuring the thickness of the human cerebral cortex from magnetic resonance images. Proc Natl Acad Sci USA. 2000; 97:11050–11055. [PubMed: 10984517]
32. Fischl B, Sereno MI, Dale AM. Cortical surface-based analysis II: Inflation, flattening, and a surface-based coordinate system. NeuroImage. 1999; 207:195–207. [PubMed: 9931269]
33. Ségonne F, Dale AM, Busa E, Glessner M, Salat D, Hahn HK, Fischl B. A hybrid approach to the skull stripping problem in MRI. NeuroImage. 2004; 22:1060–1075. [PubMed: 15219578]
34. Joyner AH, J CR, Bloss CS, Bakken TE, Rimol LM, Melle I, et al. A common MECP2 haplotype associates with reduced cortical surface area in humans in two independent populations. Proc Natl Acad Sci USA. 2009; 106:15483–15488. [PubMed: 19717458]
35. Genovese CR, Lazar NA, Nichols T. Thresholding of statistical maps in functional neuroimaging using the false discovery rate 1. NeuroImage. 2002; 15:870–878. [PubMed: 11906227]
36. Ripke S, O'Dushlaine C, Chambert K, Moran JL, Kähler AK, Akterin S, et al. Genome-wide association analysis identifies 13 new risk loci for schizophrenia. Nat Genet. 2013; 45:1150–1159. [PubMed: 23974872]

37. Simon T, Ding L, Bish J, McDonald-McGinn, Zackai E, Gee J. Volumetric, connective, and morphologic changes in the brains of children with chromosome 22q11. 2 deletion syndrome: an integrative study. Neuroimage. 2005; 25:169–180. [PubMed: 15734353]
38. Campbell LE, Daly E, Toal F, Stevens A, Azuma R, Catani M, et al. Brain and behaviour in children with 22q11.2 deletion syndrome: a volumetric and voxel-based morphometry MRI study. Brain. 2006; 129:1218–1228. [PubMed: 16569671]
39. Eliez S, Blasey CM, Schmitt EJ, White CD, Hu D, Reiss AL. Velocardiofacial syndrome: Are structural changes in the temporal and mesial temporal regions related to schizophrenia? Am J Psychiatry. 2001; 158:447–453. [PubMed: 11229987]
40. Pearlson GD, Marsh L. Structural brain imaging in schizophrenia: a selective review. Biol Psychiatry. 1999; 46:627–649. [PubMed: 10472416]
41. Kubicki M. Voxel-based morphometric analysis of gray matter in first episode schizophrenia. NeuroImage. 2002; 17:1711–1719. [PubMed: 12498745]
42. Narr KL, Bilder RM, Toga AW, Woods RP, Rex DE, Szeszko PR, et al. Mapping cortical thickness and gray matter concentration in first episode schizophrenia. Cereb Cortex. 2005; 15:708–719. [PubMed: 15371291]
43. Chow E, Ho A, Wei C, Voormolen E, Crawley A, Bassett A. Association of schizophrenia in 22q11.2 deletion syndrome and gray matter volumetric deficits in the super temporal gyrus. Am J Psychiatry. 2011; 168:522–529. [PubMed: 21362743]
44. Kunwar A, Ramanathan S, Nelson J, Antshel KM, Fremont W, Higgins AM, et al. Cortical gyrification in velo-cardio-facial (22q11.2 deletion) syndrome: A longitudinal study. Schizoph Res. 2012; 137:20–25.
45. Schaer M, Glaser B, Cuadra MB, Debbane M, Thiran J-P, Eliez S. Congenital heart disease affects local gyrification in 22q11.2 deletion syndrome. Develop Med Child Neurol. 2009; 51:746–753. [PubMed: 19416334]
46. Srivastava S, Buonocore MH, Simon TJ. Atypical developmental trajectory of functionally significant cortical areas in children with chromosome 22q11.2 deletion syndrome. Hum Brain Map. 2012; 33:213–223.
47. Thompson PM, Lee AD, Dutton RA, Geaga JA, Hayashi KM, Eckert Ma, et al. Abnormal cortical complexity and thickness profiles mapped in Williams syndrome. J NeuroscM. 2005; 25:4146–4158.
48. Hardan AY, Muddasani S, Vemulapalli M, Keshavan MS, Minshew NJ. An MRI study of increased cortical thickness in autism. Am J Psychiatry. 2006; 163:1290–1292. [PubMed: 16816240]
49. Bauman ML, Kemper TL. Neuroanatomic observations of the brain in autism: a review and future directions. Int J Develop Neurosc. 2005; 23:183–187.
50. Barkovich AJ, Chuang SH, Norman D. MR of neuronal migration anomalies. Am J Roentgenol. 1988; 150:179–187. [PubMed: 3257118]
51. Barkovich AJ, Rowley H, Bollen A. Correlation of prenatal events with the development of polymicrogyria. Am J Neuroradiol. 1995; 16:822–827. [PubMed: 7611049]
52. Kiehl TR, Chow EWC, Mikulis DJ, George SR, Bassett AS. Neuropathologic features in adults with 22q11.2 deletion syndrome. Cereb Cortex. 2009; 19:153–164. [PubMed: 18483005]
53. Robin NH, Taylor CJ, Mcdonald-mcginn DM, Zackai EH, Bingham P, Collins KJ, et al. Polymicrogyria and deletion 22q11.2 syndrome: Window to the etiology of a common cortical malformation. Am J Med Genet. 2006; 140:2416–2425. [PubMed: 17036343]
54. Gerkes EH, Hordijk R, Dijkhuizen T, Sival DA, Meiners LC, Sikkema-Raddatz B, van Ravenswaaij-Arts CMA. Bilateral polymicrogyria as the indicative feature in a child with a 22q11.2 deletion. Euro J Med Genet. 2010; 53:344–346.
55. Barkovich AJ, Guerrini R, Kuzniecky RI, Jackson GD, Dobyns WB. A developmental and genetic classification for malformations of cortical development: update 2012. Brain. 2012; 135:1348–1369. [PubMed: 22427329]
56. Schaer M, Glaser B, Ottet M-C, Schneider M, Bach Cuadra M, Debbané M, et al. Regional cortical volumes and congenital heart disease: a MRI study in 22q11.2 deletion syndrome. J Neurodevelop Dis. 2010; 2:224–234.

57. Altman D, Altman N. Further delineation of brain anomalies in velo-cardio-facial syndrome. Am J Med Genet. 1995; 175:174–175. [PubMed: 7485256]
58. Kates WR, Burnette CP, Jabs EW, Rutberg J, Murphy AM, Grados M, et al. Regional cortical white matter reductions in velocardiofacial syndrome: a volumetric MRI analysis. Biological Psychiatry. 2001; 49:677–684. [PubMed: 11313035]
59. Amelsvoort TV. Structural brain abnormalities associated with deletion at chromosome 22q11: Quantitative neuroimaging study of adults with velo-cardio-facial syndrome. Brit J Psychiatry. 2001; 178:412–419. [PubMed: 11331556]
60. Steen RG, Mull C, McClure R, Hamer RM, Lieberman JA. Brain volume in first-episode schizophrenia: systematic review and meta-analysis of magnetic resonance imaging studies. Brit J Psychiatry. 2006; 188:510–518. [PubMed: 16738340]
61. Vita A, De Peri L, Silenzi C, Dieci M. Brain morphology in first-episode schizophrenia: a meta-analysis of quantitative magnetic resonance imaging studies. Schizophr Res. 2006; 82:75–88. [PubMed: 16377156]
62. Van Erp TGM, Guella I, Vawter MP, Turner J, Brown GG, McCarthy G, et al. Schizophrenia miR-137 locus risk genotype is associated with dorsolateral prefrontal cortex hyperactivation. Biol Psychiatry. 2014; 75:398–405. [PubMed: 23910899]
63. Callicott JH, Bertolino A, Mattay VS, Langheim FJ, Duyn J, Coppola R, et al. Physiological dysfunction of the dorsolateral prefrontal cortex in schizophrenia revisited. Cereb Cortex. 2000; 10:1078–1092. [PubMed: 11053229]
64. Hashimoto T, Arion D, Unger T, Maldonado-Avilés JG, Morris HM, Volk DW, et al. Alterations in GABA-related transcriptome in the dorsolateral prefrontal cortex of subjects with schizophrenia. Molec Psychiatry. 2008; 13:147–161. [PubMed: 17471287]
65. Gur RE, Cowell PE, Latshaw A, Turetsky BI, Grossman RI, Arnold SE, et al. Reduced dorsal and orbital prefrontal gray matter volumes in schizophrenia. Arch Gen Psychiatry. 2000; 57:761–768. [PubMed: 10920464]
66. Thompson PM, Vidal C, Giedd JN, Gochman P, Blumenthal J, Nicolson R, et al. Mapping adolescent brain change reveals dynamic wave of accelerated gray matter loss in very early-onset schizophrenia. Proc Natl Acad Sci USA. 2001; 98:11650–11655. [PubMed: 11573002]

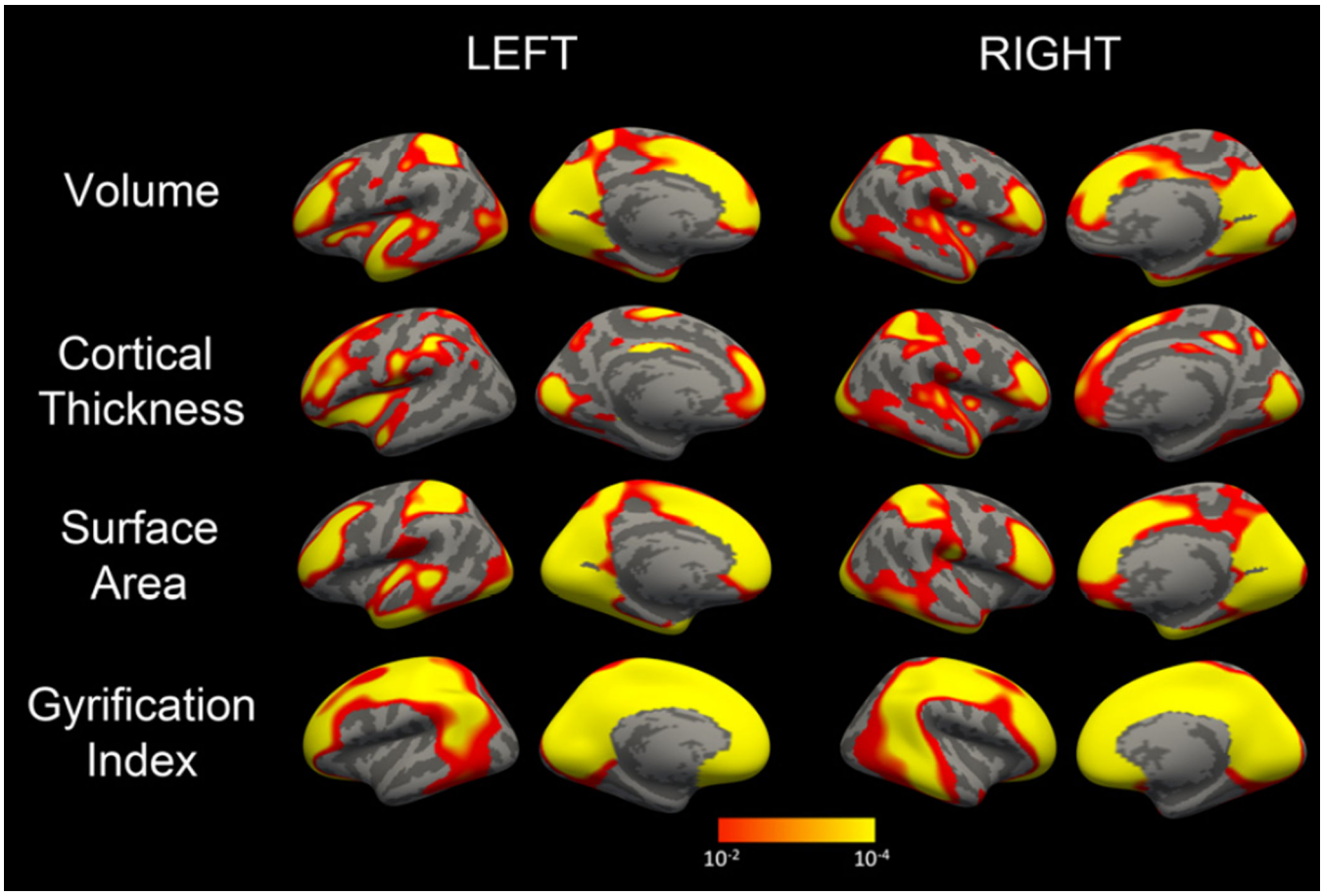

Figure 1.

Probability maps from 4-group ANOVA showing regional differences in cerebral volume (A), cortical thickness (B), surface area (C) and local gyrification index(D). Statistical maps for each hemisphere are first masked at p_{FDR}=0.05 and then displayed at an uncorrected threshold of 1.3 < -log(p) <4 for consistency.

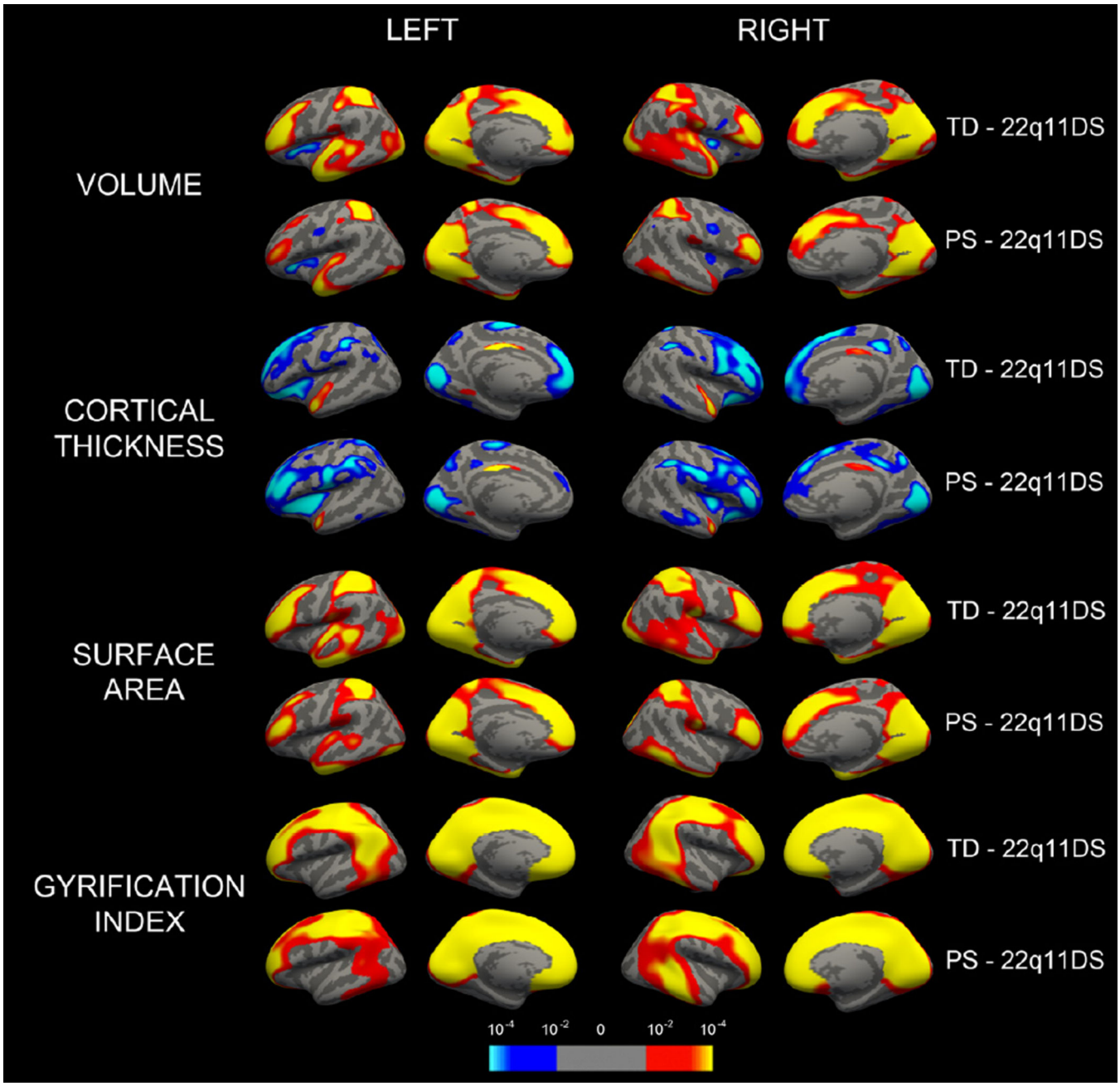

Figure 2.

Group differences driving significant changes in cortical thickness. Pairwise probability maps depicting significant increases (blue) and decreases (red/yellow) in several morphological measures as compared to typically developing (ND-TD) and idiopathic psychotic symptoms (ND-PS) groups. Statistical maps for each hemisphere are first masked at pFDR=0.05 and then displayed at an uncorrected threshold of $1.3 < -\log(p) < 4$ for consistency.

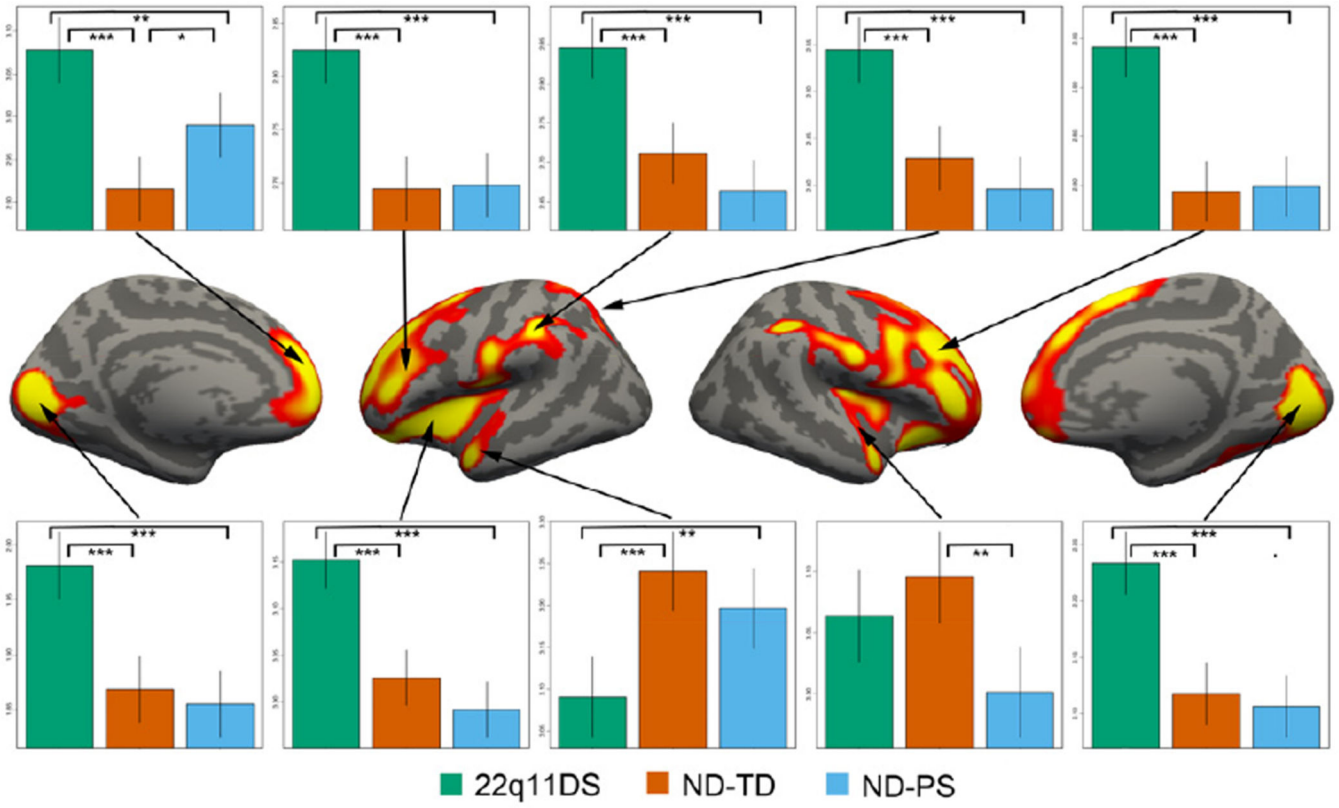

Figure 3.

Regional group differences in cortical thickness. Brain maps at center show significant vertices (global $p<0.05$) as determined via cluster threshold analysis. Plots along the periphery demonstrate group differences in mean cortical thickness for each significant cluster. Vertical lines represent 95% confidence intervals for mean cortical thickness for each group. Significant 2-way group differences are displayed with brackets (adjusted p values; *** <0.0001; ** <0.01, * <0.05).

Table 1

Demographic characteristics of the samples.

	22q11DS	ND-TD	ND-PS	p-value
N	53	53	53	
Age	20.3 (4.5)	18.6 (2.6)	18.5 (2.5)	0.01
	14.6–29.7	13.3–21.9	13.3–21.8	
Gender	27 M (51%)	27 M (51%)	27 M (51%)	1
	26 F (49%)	26 F (49%)	26 F (49%)	
Race	43 White (81%)	34 White (64%)	39 White (74%)	0.37
	7 AA (13%)	15AA (28%)	10 AA (19%)	
	3 Other (6%)	4 Other (8%)	4 Other (8%)	

ND= Non-Deleted; TD=Typically Developing; PS=Psychotic Symptoms; AA = African American. P-values are based on ANOVA for age and chi-square test for categorical variables.

Table 2

Mean (SD) global measures by group.

	Cortical Volume (mm^3)	Cortical Thickness (mm)	Surface Area (mm^2)	lGI
ND-TD	525788 (68511)	2.69 (0.09)	176346 (19263)	3.01 (0.13)
ND-PS	543620 (60455)	2.68 (0.11)	171569 (19535)	3.01 (0.21)
22q11DS	495180 (56334)	2.75 (0.10)	157533 (19192)	2.88 (0.17)
p-value	0.0009	0.0004	<0.0001	0.0001

ND=Non-deleted; TD= Typically developing; PS=Psychotic symptoms; lGI = Local gyrification index